Progress in Materials Science 124 (2022) 100873

Contents lists available at ScienceDirect

Progress in Materials Science

journal homepage: www.elsevier.com/locate/pmatsci

Snapshot Review

On the potential of aluminum crossover alloys

Lukas Stemper [a], Matheus A. Tunes [b], Ramona Tosone [c], Peter J. Uggowitzer [d,*], Stefan Pogatscher [d]

[a] Christian Doppler Laboratory for Advanced Aluminum Alloys, Chair of Nonferrous Metallurgy, Montanuniversitaet Leoben, Franz-Josef-Straße 18, 8700 Leoben, Austria
[b] Materials Science and Technology Division, Los Alamos National Laboratory, Los Alamos, NM 87545, United States
[c] AMAG Rolling GmbH, Lamprechtshausener Straße 61, 5282 Ranshofen, Austria
[d] Chair of Nonferrous Metallurgy, Montanuniversitaet Leoben, Franz-Josef-Straße 18, 8700 Leoben, Austria

ARTICLE INFO

Keywords:
Aluminum alloys
Crossover alloys
Strength
Formability
Ductility
Sustainability
AlMgCu
AlMgZn
AlMgZn(Cu)

ABSTRACT

For almost a century commercial aluminum alloys were developed and optimized for high performance in a specific and narrow range of application, which commonly coincides with their industrial classification. Overcoming the limitations associated with the modern lightweighting concept requires new alloy design strategies that offer an expanded property portfolio with a better trade-off between formability and achievable strength. The associated materials would be key to circumventing the need for a multi material mix that diminishes the recyclability of the final product. This review summarizes current knowledge about a new class of materials, "crossover alloys", that combine advantageous properties normally limited to certain classes of commercial aluminum alloys. It focuses on the crossover alloys AlMg/AlCuMg (5xxx/2xxx) and AlMg/AlZnMg(Cu) (5xxx/7xxx). Recently available research data provides indications for superior formability with simultaneously high age-hardening potential, which may pave the way for broader industrial application in the foreseeable future. Because these new alloys exhibit Mg as their major constituent but are – in contrast to commercial AlMg alloys – age hardenable, they do not fit into the current alloy classification scheme. This review formalizes crossover alloys as a potential new aluminum alloy class which features an innovative alloy design methodology.

1. Introduction

Global warming and climate change have been identified as global threats to mankind. Their undesired and harmful consequences are strongly correlated with the accelerated growth of the transportation sector over the last few decades, which is responsible for increasing CO_2 emission levels [1,2]. The increasing economic implications and rising political awareness of the climate change challenge have boosted research and development activities to address it, but definitive solutions have not yet been reached [3,4].

From a holistic point of view, significant improvements in mitigating greenhouse gas emissions require an overall decrease in energy consumption. Even though new automotive technologies like those featured in electric cars can to some extent enhance fuel efficiency in traffic and transportation [5–9], from an engineering perspective major energy savings also require that substantial improvements be made to the design of vehicles and the materials used to make them. Consequently, the development of new materials which address the increased demand for both appropriate properties and sustainability must become a major focus.

* Corresponding author.
E-mail address: peter.uggowitzer@mat.ethz.ch (P.J. Uggowitzer).

https://doi.org/10.1016/j.pmatsci.2021.100873
Received 11 June 2021; Received in revised form 29 September 2021; Accepted 29 September 2021
Available online 1 October 2021

Lightweighting by deploying low-density materials such as aluminum alloys as substitutes for high-density materials such as steel is a well-established [10–12] but insufficient approach to mitigating greenhouse gas emissions, because the applicability of commercially available aluminum alloys is restricted due to their usually limited property spectrum. In addition, multiple operational demands and engineering criteria, in particular those related to material's formability and strength [13], still require the utilization of several different material concepts which limit product recyclability [14–17].

Overcoming the limitations associated with state-of-the-art lightweighting concepts requires the development of new alloy design strategies capable of delivering an extended property portfolio which features both good formability during processing and high strength in use. The associated materials would be key to circumventing the need for a multi material mix that diminishes the recyclability of the final product.

2. Crossover alloying

Although most commercial aluminum alloys might exhibit a limited spectrum of properties, they are designed for high performance in a specific and narrow field of use. Their main purpose is often predefined by their major alloying constituents [18], which also determine their industrial classification, i.e. Cu in 2xxx-series alloys (AlCu(Mg) alloys with a Cu/Mg ratio > 1), Mg in 5xxx-series alloys (AlMg(Mn) alloys with a Mg/Mn ratio > 1) or Zn in 7xxx-series alloys (AlZnMg(Cu) alloys with a Zn/Mg ratio > 1). Note that alloy compositions are presented in wt.% throughout this review, and scientific abbreviations are used to refer to certain alloy classes (for example, "AlCuMg alloys" indicates 2xxx-series alloys). Within these classes, materials' properties vary over a relatively wide range (depending on the exact alloy composition and condition), but there is an overall trend, at least in some distinct attributes, compared to other alloy classes. In terms of mechanical performance, commercial aluminum alloys usually offer poor formability during processing but high in-use strength [19–21] or good formability but only moderate final strength [21,22]. To address this longstanding trade-off between formability and achievable strength, which is very significant for future aluminum-based materials, it is reasonable to identify alloys or classes of alloy which outperform others in at least one of the desired material property categories.

Alloys corresponding to the AlZnMg(Cu) classification, for example, offer the highest achievable yield strength levels [18,23–31], closely followed by AlCu(Mg) alloys [18,32–37]. Commercial AlMgSi alloys exhibit sufficient bake hardening potential, surface quality and corrosion resistance [10,18]. Since they also offer good levels of fracture elongation in soft condition [38–44], they currently hold around 60 % of the aluminum-based materials market [15]. However, tuning AlMgSi alloys for higher in-use strength by either increasing the Si content [45], adding additional alloying elements such as Zn [46] or performing a pre-aging treatment [40] results in significantly impaired performance during forming. Several attempts have been made to enhance the forming capability of these alloys [39,47,48] but a definitive and reliable approach is still pending. As opposed to AlMgSi alloys, commercial AlMg(Mn) alloys exhibit a high level of ductility and work hardenability [18,49,50], which makes them more suitable for complex forming operations [21,22]. However, surface deterioration via formation of stretcher strains and only moderate strength – these alloys cannot be age hardened – limit their broad application [51–54].

Given the limitations of state-of-the-art commercial aluminum alloys described above, it is indicated that new alloys requiring good formability during processing and high strength in use should combine the beneficial formability of AlMg(Mn) alloys with the good strengthening ability of AlCu(Mg) or AlZnMg(Cu) alloys. Bringing this merger about by alloy design – thus creating a "crossover" between different alloy classes – has attracted the attention of the metallurgical community, and promising results have recently been reported. Initially, normally non-heat-treatable AlMg alloys were chosen with the aim of establishing a high level of formability, as work hardenability and uniform elongation tend to increase with increasing Mg content [55]. Subsequently, sufficient age hardening potential was established by adding alloying elements such as Cu and/or Zn, which tend to form composition-dependent hardening precipitates upon aging. Because Mg is consumed by all major precipitates in the AlMgZnCu system, relatively high levels of Mg (Mg/

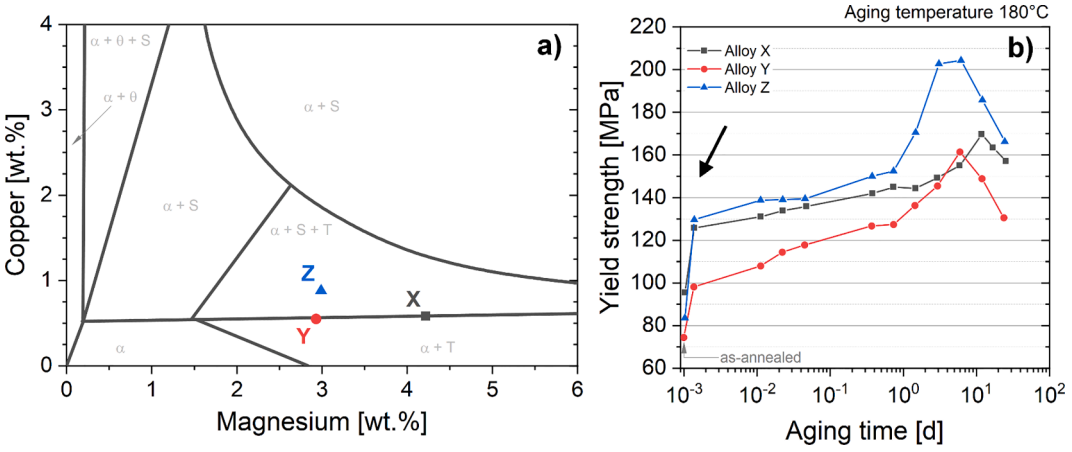

Fig. 1. (a) Equilibrium phase diagram Al-Cu-Mg at 190 °C. (b) Evolution of yield strength in AlMgCu alloys with varying Cu/Mg ratios. Reprinted from [60] with permission from the JIM (Japan Institute of Metals and Materials).

Zn > 1, Mg/Cu > 1) are required to ensure an adequate amount of this element in solid solution to maintain both a good formability in pre-aged conditions and a sufficient damage tolerance upon final heat treatment.

As these new alloys exhibit Mg as their major constituent but, in contrast to commercial AlMg alloys, are indeed age hardenable, they do not fit well into the current alloy classification scheme. Hence the proposal was made to call them **"crossover alloys"** [14,56,57]. This review provides a comprehensive overview of these new crossover alloys, and consolidates crossover alloying as an innovative design concept in metallurgy.

3. AlMgCu crossover alloys

While AlCu(Mg) alloys (Cu/Mg ratio > 1) are well established for commercial use as 2xxx-series alloys, adding Cu to AlMg alloys (Cu/Mg ratio ≪ 1) has only recently attracted the attention of the metallurgical community. This type of alloy was mentioned in a publication for the first time in the early 1990s, as preventing softening during the paint bake process [58]. The hardening response observed during heat treatment (175 °C/30 min) of pre-deformed (2%) sheets successfully counteracted recovery processes.

Early studies by Ratchev et al. [59,60] investigated the hardening response during aging in the range of 60 °C to 180 °C in several AlMgCu alloys exhibiting Cu/Mg ratios of between 0.14 (Alloy X in Fig. 1) and 0.29 (Alloy Z in Fig. 1). Upon aging at 180 °C, all the alloys investigated exhibited an initial jump in yield strength ($\Delta Rp_{0.2} = 20 - 40$ MPa), followed by a linear increase until peak hardness ($\Delta Rp_{0.2} = 70 - 120$ MPa) was reached (Fig. 1b). This hardening characteristic was found to be similar to that of AlCu(Mg) alloys [61,62] and was attributed to precipitation of the S-phase and its precursors following the sequence:

SSSS (supersaturated solid solution) → Cu/Mg clusters (GPB-zones) → S'-phase → S''(S) (Al_2MgCu) [59]

The initial jump in the yield strength (see black arrow in Fig. 1b) is attributed to rapid formation of Cu/Mg clusters [61,62] which is significantly faster and more pronounced at higher Cu/Mg ratios, but less affected by temperature variations at higher temperature levels (140 – 180 °C). At a low Cu/Mg ratio and low aging temperature, the peak hardness – which is attributed to S'-precipitates – shifts to longer aging times. In contrast to thermodynamic calculations (see Fig. 1a), T-phase ($Mg_{32}(Al,Cu)_{49}$) hardening was not observed, which may result from impurities (Si, Fe, Mn) stabilizing the S-phase [59,60]. Even though the S-phase has been identified as the major hardening precipitate in aluminum alloys containing significant amounts of (e.g.) Mg and Cu, its precipitation and development are still subjects of ongoing research and debate in the areas of both AlCuMg alloys [63–65] and AlMgCu alloys [66–69].

The beneficial effect of Cu in AlMg alloys and the associated hardening response to avoid softening of pre-deformed sheets depends on the recrystallization / solution annealing and aging treatment used, but is also linked to the level of deformation applied before the final aging treatment. This is discussed in detail below.

In order to establish sufficient age hardening potential, the supersaturation of solutes and vacancies is required. It renders commonly utilized recrystallization annealing treatments at medium temperatures (black lines in Fig. 2a and Fig. 2b; for details see figure caption) insufficient if > 2% pre-deformation is applied [70]. If adequate high-temperature solutionizing and quenching (red lines in Fig. 2a and Fig. 2b) are performed, softening during subsequent heat treatment can be significantly mitigated [71] or even prevented up to either 5% [70] or 10% [72] pre-deformation if the alloy composition and heat treatment parameters are appropriately adjusted. Medrano et al. [73] revealed that additions of (only) 0.12 at% of Cu are sufficient to establish a rapid hardening response at the initial stage of aging at 200 °C. Strengthening particles (clusters/GPB-zones) were observed to exhibit similar size and geometry, but they incorporate a significantly lower amount of Cu compared to commercial AlCuMg alloys after 20 min of aging, thus explaining

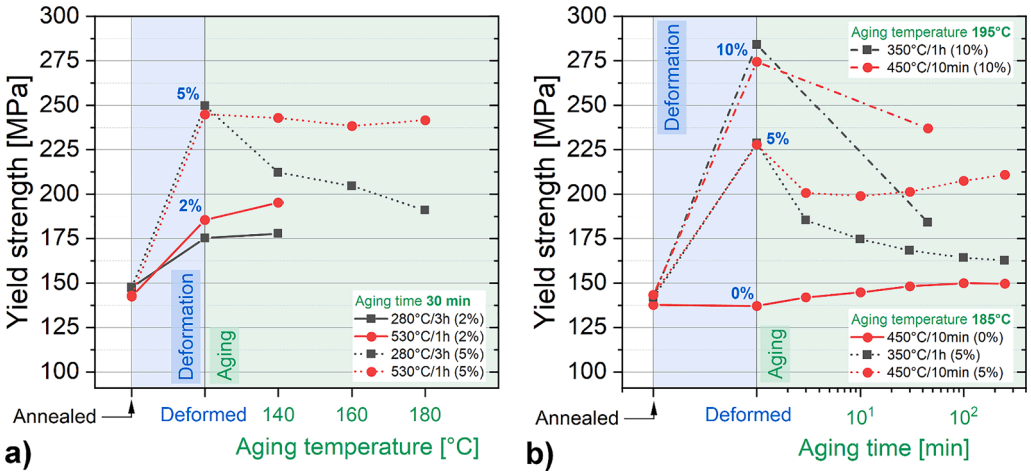

Fig. 2. Evolution of yield strength with applied processing/aging. (a) AlMg4.6Cu0.54; values correspond to 30 min of aging [70]. (b) AlMg5.4Cu0.33, batch-annealed (350 °C/1 h, slow cooling, black lines), solution heat treated (450 °C/10 min, fast cooling, red lines) [71]. Reprinted from [70,71] with permission from Elsevier. Figures are slightly modified for easier readability.

the relatively high particle density regardless of the low bulk Cu content [73]. Negative effects of natural aging such as deteriorated hardenability or limited formability – known from commercial AlMgSi alloys [74–77] – are not observed in AlMg alloys which contain Cu [71,78,79].

Zhang et al. [80,81] investigated the potential of AlMgCu crossover alloys for processing via equal channel angular pressing (ECAP). An AlMg4.3Cu1.2 alloy was artificially aged to under-, peak- and over-aged condition before being subjected to several ECAP passes at 180 °C. While coarse hardening precipitates (S-phase or its precursors) in peak-aged condition fractured and dissolved during processing, small precipitates in under-aged condition dissolved similarly but re-precipitated, resulting in significantly higher yield stress caused by strengthening contributions from dislocations and grain boundaries but also from beneficial interactions of dislocations with solutes and re-precipitated hardening phase. Post-ECAP aging had no effect on initially peak-aged samples but resulted in a significant loss of strength in initially under-aged samples [80,81].

Because adding Cu has been shown to prevent Mg-migration towards grain boundaries and also to suppress the formation of β-Phase (Al_3Mg_2) in favor of Cu-bearing hardening phase, AlMgCu alloys offer enhanced resistance against intergranular corrosion (IGC) if an adequate solutionizing treatment is applied [70]. While susceptibility to pitting corrosion was observed to be neither improved nor degraded compared to a Cu-free reference alloy, resistance to filiform corrosion was reported to be enhanced by Cu addition [71].

4. AlMgZn crossover alloys

While η-precipitates are the dominant hardening phase in commercial AlZnMg(Cu) alloys (corresponding to the class of 7xxx-series alloys) [82], strengthening by T-phase is not widely established. Even though this ternary phase has been known since 1936 and was included in Al-Mg-Zn equilibrium phase diagrams by Köster et al. [83,84], interest in potential T-phase hardening was only minor during the twentieth century [82,85–89]. This may be because alloys of commercial interest, which were supposed to consist of only T-phase and aluminum matrix (under equilibrium condition), were also observed to harden only via η or its precursors [89]. Therefore it was suggested that T-phase tends to evolve from η-particles only at higher temperatures (> 200 °C) [89,90], as opposed to direct formation upon aging, since other T-precursors (with deviating crystal structure from equilibrium T) are not known [89]. Recently, however, sole T-phase hardening in AlZnMg(Cu) alloys with Zn/Mg ratios ≤ 2.2 has attracted increased attention [91,92]. Because the AlMgZn crossover alloys investigated here contain Mg in excess (Zn/Mg ratios < 1), hardening by T-phase and/or its precursors can be similarly expected.

Today it is generally accepted that under equilibrium conditions, the T-phase (denoted as $Mg_3Zn_3Al_2$, $Mg_{32}(Al,Zn)_{49}$ or $Mg_{32}Zn_{31.9}Al_{17.1}$) exhibits a body-centered cubic crystal structure containing 162 atoms in its unit cell [93–96]. It can be identified according to its distinct reflection spots within the aluminum matrix along the ⟨001⟩ zone axis, exposing the characteristic T-phase diffraction spots at the 2/5 and 3/5 ⟨022⟩ Al positions [97]. The precipitation sequence of the T-phase is still a matter of debate, as the Al and Zn atoms can randomly occupy Al/Zn substitutional lattice sites in the T-phase unit cell [93]. Therefore the precipitation sequence in AlMgZn crossover alloys is strongly dependent on a given alloy composition [90,93,98–101]. This has also been observed in AlZnMg(Cu) alloys hardened by co-precipitation of η- and T-phase [91,92,102,103]. Consequently, a wide variety of possible precipitation sequences have been proposed for the Al-Mg-Zn system; they are summarized in Table 1.

According to the findings of Bigot et al. [98] in an AlMg4.9Zn3.2 alloy, precursor T'- and equilibrium T-phase exhibit similar crystal structures (and therefore similar electron-diffraction signals) and similar orientation relationships with the Al matrix, but can be distinguished by their chemical compositions, which were found to be independent of particle size. However, determining the evolution state of T-phase particles by chemical constitution may be applied to a single alloy composition only, rather than being deployed for a general comparison, because the equilibrium composition of T-phase is probably affected by overall alloy constitution due to random occupancy of Al/Zn lattice sites [91]. More recent investigations into the precipitation sequence in an AlMg5.1Zn3.0(Cu0.15) alloy by Hou et al. [105] resorted to the level of coherency to identify the evolution state of precipitates. Two different types of GP zone were observed at early stages of aging. While fully coherent solute clusters without distinct diffraction signals were denoted as GPI zones, slightly larger, but still fully coherent precipitates with distinct diffraction signals were assigned as GPII (T'') zones. Because T'- and T-precipitates exhibit similar crystal structures, as observed by Bigot et al. [98], they were distinguished by their respectively semi-coherent and incoherent interfaces with the matrix. It is important to emphasize that GPI and GPII zones in AlMgZn crossover alloys do not correspond to GPI and GPII zones in commercial AlZnMg(Cu) alloys [82,107]. Slightly different precipitation behavior was observed by complementary deployment of atom probe tomography (APT), transmission electron microscopy (TEM) and density functional theory (DFT) techniques conducted in-house. We recently proposed that transient η'-surrogates might be involved in the transformation from GPI zones into T' in an AlMg4.7Zn3.6 alloy [106].

Table 1
Proposed precipitation sequences for the η and T phases within the Al-Mg-Zn system.

a)	SSSS → GP (Guinier-Preston) zone → intermediate η' →equilibrium η → equilibrium T	[90]
b)	SSSS → solute–vacancy-complex → GP zone → intermediate η' or T' →equilibrium η or T	[99]
c)	SSSS → GP zone → intermediate η' or T' →equilibrium η or T	[101]
d)	SSSS → GP zone → intermediate T' →equilibrium T	[104]
e)	SSSS → GPI zone → GPII zone (T'') → intermediate T' →equilibrium T	[105]
f)	SSSS → GPI zone →(transient η' →) intermediate T' →equilibrium T	[106]

SSSS (supersaturated solid solution).

Although the recent interest in the crossover AlMgZn alloys can be attributed to their good hardening potential, Zn addition (in relatively low amounts) was first utilized to enhance the resistance of commercial AlMg alloys to several corrosion mechanisms (see Table 2). This beneficial effect has been attributed to the suppression of highly anodic β-phase at grain boundaries in favor of less anodic T-phase upon stabilization and sensitization [108–113]. In addition to improved corrosion resistance, small additions of Zn (< 1 wt%) were also reported to increase the yield strength (see Fig. 3a) after stabilization treatment (250 °C/1 h). This can be explained by the synergistic effects of increased solid solution strengthening and hardening precipitates [109,112].

Increasing the Zn content and applying a solutionizing treatment (rather than recrystallization annealing) has been shown to cause a significant increase in yield strength upon both artificial and natural aging [106,114–119].

The hardening response upon artificial aging has been found to be caused mainly by precipitation of T-phase and/or its precursors [114,115,117–119]. Cao et al. [115] investigated the artificial aging behavior of an AlMg5.2Zn2.0(Mn0.2) alloy at 180 °C, revealing an incubation period of approximately 2 h before hardness increased towards peak level after 24 h of aging. Yun et al. [117] observed hardening only at Zn levels higher than 3 wt% in an AlMg5 alloy upon aging at 120 °C (compare Fig. 3b and c). In contrast, however, hardening incubation was much shorter and the overall hardness level was significantly higher. The latter results are consistent with the findings reported in [118], where the aging behavior of an AlMg5.0Zn3.8(Mn0.8) alloy at a temperature range of 75 – 200 °C was investigated. Both the earliest hardening onset (approximately 1 h) and the greatest hardness gain were found at lower temperatures (100 °C), probably due to a beneficial tradeoff between nucleation and growth of hardening phase [118]. On the other hand, it has also been reported that hardening initiates only after approximately 16 h at 125 °C in an AlMg4.7Zn3.5(Mn0.4) alloy, which resulted in a peak-aging time of 9 days [119].

In contrast to the works mentioned above, which observed sole T-phase hardening in AlMgZn crossover alloys only, investigations by Zhu et al. [121] on Fe-rich (1.5 wt%) AlMg5(Mn0.5) alloys manufactured by high pressure die casting (HPDC) revealed that Zn addition (up to 3 wt%) resulted in sole η-phase hardening if a low-temperature heat treatment (430 °C/60 min + water quenching + 120 °C/16 h) was applied.

All these results indicate that alloy composition and aging strategy have to be carefully matched to establish a sufficient and optimal hardening response. In addition, inconsistencies in the hardening behavior between the reported alloys might be attributed to the presence and number of additional alloying elements and impurities such as Mn, Fe, Si, Cr, Ti, Zr, Sc, etc., which can affect nucleation of precipitates and thus facilitate [122] or degrade [123] the hardening response.

In contrast to the hardening behavior in most commercial AlZnMg(Cu) alloys [92], peak hardness in T-hardened AlMgZn crossover alloys shifts to longer aging times, usually between 24 h [115] and 9 days [119] upon single-step aging, but this depends on the alloy composition and heat treatment parameters. Because processing time – especially the aging time in the final heat treatment stage – is a key aspect for industrial applicability, efforts must be made to accelerate the hardening response. Performing a low-temperature pre-aging treatment (from 3 h to 12 h at 80 °C to 100 °C) prior to the final high-temperature aging stage has been shown to significantly accelerate the hardening response, thus results in a shortening of the total time to reach peak hardness. This has been attributed to the formation of stable precursors in high number density, acting as preferential nucleation sites for subsequent development of the hardening phase [97,118,119,124,125]. Minor deformation (2%) after pre-aging was also reported to have a boosting effect on the hardening response; this has been attributed to enhanced mobility of solutes facilitated by dislocations introduced by deformation [106].

Pre-aging and natural aging caused both an increase in yield strength and a shift of the onset of serrated flow to higher strain levels (see Fig. 3b). This is attributed to both the strengthening ability and the vacancy-trapping nature of small coherent Mg-Zn clusters/GPI zones [106,114]. Increased levels of Zn (up to 5 wt%) have also been shown to have no deteriorating effect on elongation in AlMg alloys with low Mg content (≤ 5 wt%) in either as-quenched [117] (see Fig. 3c) or pre-aged condition [106], regardless of their potential higher strength. Geng et al. [126] also observed a partial suppression of Lüders elongation in a pre-aged (485 °C/10 min + water quenching + 80 °C/12 h) AlMg5.1Zn3.0 alloy which is not seen in AlMg4.6Cu0.15 in soft-annealed (450 °C/1 h) condition.

Based on the indications for such alloys' beneficial forming performance in pre-aged condition, Stemper et al. [106] compared two pre-aged (PA) crossover alloys – AlMg4.7Zn3.6 (black line in Fig. 4)) and AlMg4.7Zn3.6Cu0.6 (red line in Fig. 4) – with a commercial EN AW-5182 alloy in its dedicated forming condition (soft annealed, blue line in Fig. 4), by plotting the strain hardening rate (SHR) over plastic stress (σ-σ_0) for their corresponding true stress–strain curves as an indication for stretch-formability.

The observed higher level of SHR over the full range of plastic stress and the flatter slope of the curves were linked to enhanced formation and inhibited annihilation of dislocations, respectively, thus indicating a better performance during stretch-forming commonly applied in the manufacturing of automotive sheets [106,119,127–129]. A similar conclusion arises by comparing the

Table 2
Effect of Zn addition on the corrosion resistance of crossover alloys. Vertical arrows indicate an improvement in corrosion resistance.

Zn [wt.%]	Mg [wt.%]	Processing*	Stabilization treatment	Sensitization treatment	Corrosion resistance**	Ref.
0.68–0.70	4.7	H, HR, IA, CR	110 °C/2 h	200 °C/24 h	↑ (exfoliation)	[108]
0.00–1.00	5.8	H, HR, IA, CR	250 °C/1 h	100 °C/7 d	↑↑ (IGC)	[109]
0.00–1.00	5.8	H, HR, IA, CR	250 °C/1 h, 1 %	100 °C/7 d	↑↑ (IGC), ↑↑ (SCC)	[112]
0.00–0.78	4.5	H, HR, CR	200 °C	7 d	↑↑ (IGC), ↑↑ (PC)	[111]
0.70–1.50	4.0–7.0	H, HR, CR, IA, CR, SA	200–260 °C/1–24 h	150 °C/3 d	↑↑ (SCC)	[120]

* H: Homogenization; HR: hot rolling; IA: intermediate annealing; CR: cold rolling; SA: solution annealing.
** ICG: intergranular corrosion; SCC: stress corrosion cracking; PC: pitting corrosion.

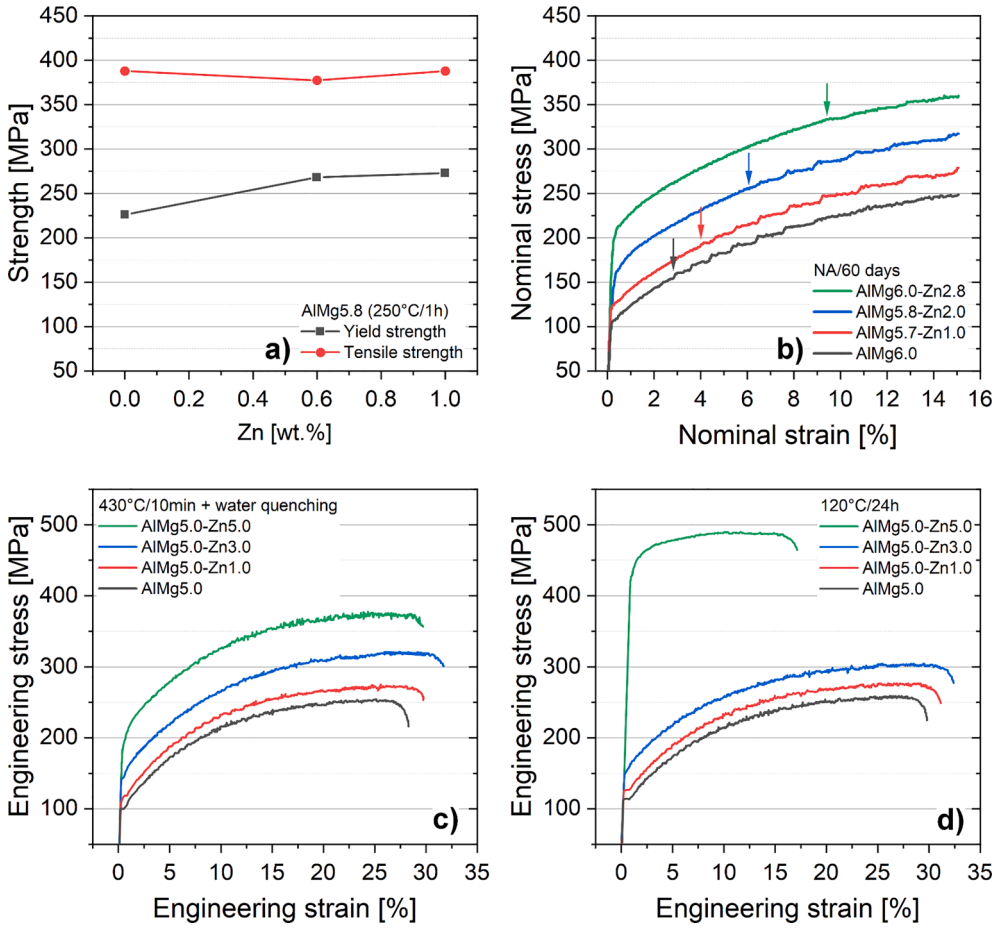

Fig. 3. Effect of Zn content on the yield strength of crossover alloys. Plots in (a) after stabilization (250 °C/1 h) [109]; (b) after solutionizing and natural aging for 60 days, where onset of serrated flow is shifted to higher strain levels [114]; (c) engineering stress–strain curves after solution annealing (430 °C/10 min) and quenching [117]; (d) engineering stress–strain curves after aging for 24 h at 120 °C [117]. (Reprinted from [109,114,117] with permission from Elsevier and Trans Tech Publications, Ltd.)

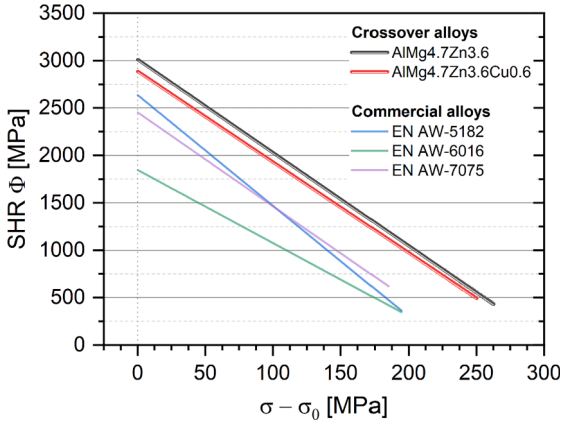

Fig. 4. Kocks-Mecking-plots [127] of AlMg4.7Zn3.6 (PA 100 °C/3h, black line), AlMg4.7Zn3.6Cu0.6 (PA 100 °C/3h, red line), EN AW-5182 (soft annealed, blue line), EN AW-6016 (PA 100 °C/5h, green line) and EN AW-7075 (PA 120 °C/2h, pink line). Both crossover alloys exhibit a significantly higher level of strain hardening rate over the full range of plastic stress indicating a more beneficial stretch-forming performance. σ_0-values correspond to $Rp_{0.2}$ (PA) shown in Table 3. Reprinted from [106] with permission from Elsevier. Note that figure has been slightly modified for easier readability.

results assessed from commercial alloys EN AW-6016 (green line in Fig. 4) and EN AW-7075 (pink line in Fig. 4) in comparable heat treatment states (for details see figure caption). Note that these conditions have been chosen as both alloys require such processing prior to forming to achieve their intended strength in use upon final paint bake treatment (20 min at 185 °C) [39,46,130–132]. However, it has to be mentioned that comprehensive experimental data addressing the formability of crossover alloys has not been yet published and requires further research. Nevertheless, investigations of the paint bake response $\Delta Rp_{0.2}$ of the alloys shown in Fig. 4 (summarized in Table 3) also reveal a significant hardening potential of crossover alloys, which can be further tailored by minor alloy modification (for details see section 5).

As previously mentioned, small additions of Zn (< 1 wt%) can enhance the resistance of AlMg alloys to IGC given adequate heat treatment (stabilization). By increasing the levels of Zn and applying artificial aging treatments to exploit the full hardening potential, the susceptibility of AlMgZn alloys to IGC is significantly increased due to the non-beneficial galvanic coupling between precipitate free zones (PFZ) and grain boundary precipitates (GBP) [134]. Increasing the Zn/Mg ratio (at levels below 1) [135], adding Cu (for details see the next section) [135] or applying a retrogression and re-aging (RRA) treatment [136] (first introduced by Cina et al. [137] for AlZnMg(Cu) alloys) have been shown to generate narrower PFZs and discontinuous GBPs, thus enhancing IGC resistance.

Beside their beneficial strengthening ability T-phase particles in overaged AlMgZn crossover alloys were also observed to exhibit a significant resistance to heavy ion irradiation (Pb^{+}). This was attributed to the high phase fraction and advanced chemical complexity of the hardening phase, and makes such alloys potential candidates for utilization in vehicles intended for space exploration [56].

5. AlMgZn(Cu) crossover alloys

Because adding both Zn and Cu has been shown to have beneficial effects on the corrosion susceptibility and the hardening capability of AlMg alloys, combined addition of these elements was also investigated. While corrosion was the major focus of the earlier studies, recent work has aimed to exploit the hardening potential of AlMgZn(Cu) alloys.

Carroll et al. [138,139] investigated the effect of different Cu levels (0.075 – 0.24 wt%) on the formation and corrosion impact of potential secondary phases in Zn-modified (0.6 wt%) 5083 alloys upon extensive sensitization (165 °C/175 – 350 h). While at lower Cu additions only Cu-enriched T-phase ($Mg_{32}(Al, Zn, Cu)_{49}$) was observed at grain boundaries, alloys with high Cu levels contained a significant amount of corrosion-prone S-phase in the grain interior. Tensile tests on alloy samples containing Zn and Cu in a corrosion-promoting environment indicated that well-balanced Cu addition significantly counteracts the susceptibility to stress corrosion cracking (SCC) observed in Cu-free AlMgZn alloys, as long as the formation of S-phase is inhibited. Even though these alloys showed lower ductility compared to commercial 5083 in a non-corrosive environment (dry air) upon sensitization, they outperformed them in a corrosive (aqueous NaCl) environment [138,139].

Systematic investigations of the hardening response and the associated microstructural evolution in AlMgZn(Cu) alloys started rather recently, in 2016. Cao et al. [115] addressed the effects of combined Zn- and Cu addition by investigating the impact of gradually increasing Zn levels (0.6 – 1.9 wt%) in an AlMg5.2Cu0.45 alloy upon aging at 180 °C (Fig. 5a). At early aging stages, the effect of Zn was less pronounced because rapid hardening (I) via the formation of Mg-Cu clusters (similar to AlCuMg [61,62] or AlMgCu [59,60] alloys) was found to dominate over that of Mg-Zn clusters. With increasing Zn content (up to 1.9 wt%) the incubation time for T-phase precipitation was shortened (II) and peak hardness (III) was both shifted to shorter aging times and significantly enhanced (compare black and green lines in Fig. 5a) by subsequent development of the T-phase, thereby increasing the Cu/Mg ratio in the matrix and thus accelerating the formation of the S-phase. The maximum strength was attributed to the synergistic effects of both T- and S-phases (see Fig. 6b). Due to the relatively small Zn content and the resulting low Zn/Mg ratio, the absolute increase in hardness is only moderate under the applied aging conditions seen in Fig. 5b [115,118,119].

However, these findings contrast with the results of Tang et al. [140], who investigated the hardening response of an AlMg5.0Zn3.0 cast alloy containing a large amount of Cu (1 wt%) during single-step artificial aging experiments at temperatures between 120 °C and 175 °C. While peak hardness was found to be almost independent of the aging temperature and was attributed to small globular GPII zones (T'') and large, rod-shaped Cu-enriched T'-particles, the time required to reach the highest strength levels was significantly shorter (4 h) at 175 °C when compared to aging at 120 °C (125 h). Higher aging temperatures were assumed to promote the formation of T' over GPII (T'') due to enhanced diffusion of solutes (especially Cu), thus increasing the average precipitate size and finally resulting in a deteriorated ductility and a decreased impact toughness [140].

For AlMgZn alloys with lower Cu levels (0.15 – 0.6 wt%), applying a low-temperature pre-aging treatment (3 h to 48 h at 80 °C to

Table 3
Change in yield strength of alloys shown in Fig. 4 upon paint bake treatment.

Alloy	$Rp_{0.2}$ (PA*) [MPa]	$Rp_{0.2}$ (PB**) [MPa]	$\Delta Rp_{0.2}$ [MPa]	$\Delta Rp_{0.2}$ [%]	
Crossover alloys					
AlMg4.7Zn3.6	157	204	47	30	[106]
AlMg4.7Zn3.6Cu0.6	226	353	127	56	[106]
Commercial alloys					
EN AW-5182	159	159	0	0	[106]
EN AW-6016	154	242	88	57	[133]
EN AW-7075	429	508	79	18	[130]

* PA: Pre-aged condition (for details see caption of Fig. 4).
** PB: Paint bake condition (185 °C/20 min).

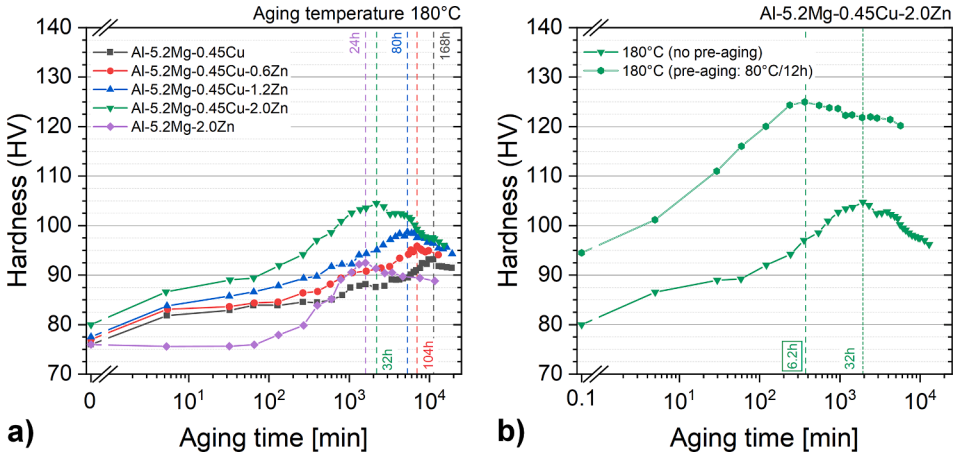

Fig. 5. (a) Hardening response of AlMg alloys with varying Zn- and Cu content during aging at 180 °C [115]; (b) Hardening response of AlMg5.2Zn2.0Cu0.45 upon aging at 180 °C without (green rectangles) and with (green dots) prior pre-aging (80 °C/12 h) [97]. Reprinted from [97,115] with permission from Elsevier.

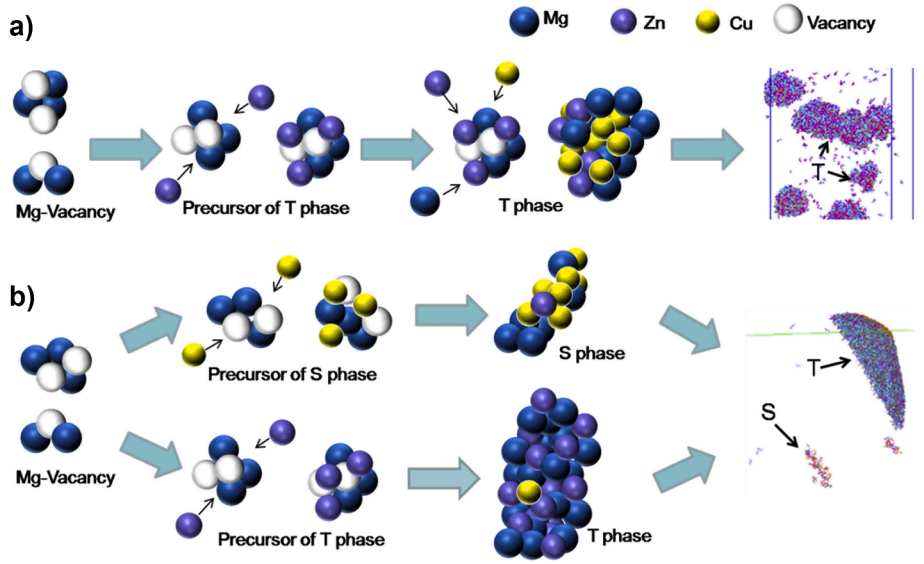

Fig. 6. Schematic illustration of precipitate development in AlMg5.2Zn2.0Cu0.45 upon aging at 180 °C with (a) and without (b) prior pre-aging (80 °C/12 h) [97]. Reprinted from [97] with permission from Elsevier.

100 °C) prior to subsequent high-temperature final aging (140 – 180 °C) was found to significantly accelerate the hardening response during the second aging stage, shift the peak hardness to earlier times [97,118,119,125] and generate higher hardness levels [97,119,125] (see Fig. 5b) due to major changes in the microstructure. While peak hardness was attributed to coarse, lath-like T-phase and needle-shaped S-phase in low density if no pre-aging is applied, the microstructure in pre-aged and subsequently peak-aged condition consists of finely-dispersed, equiaxed T-phase particles in higher density. Although the T-phase particles exhibit similar crystal structures in both conditions, their chemical compositions were found to differ significantly. It is assumed that low temperature pre-aging promotes the formation/nucleation of precursors (GP zones) by vacancy-assisted diffusion; they are able to grow and evolve into Cu-enriched T-phase upon subsequent high-temperature aging by solute attachment of Zn and Cu, thus suppressing S-phase formation (see Fig. 6a). It seems reasonable to assume that adding Cu in larger quantities [140] will – if high-temperature single-step aging is applied – have an effect similar to that of the precursors present after pre-aging in low-Cu AlMgZn alloys [97,118,119,125].

These results were confirmed by Hou et al. [141], who followed a similar approach to Cao et al. [115] and investigated the effect of increasing Zn levels (1 – 4 wt%) in an AlMg5.1ZnXCu0.15 alloy during two-stage aging treatments by means of APT analysis. They found an enhanced and accelerated hardening response (during both natural aging and second-stage artificial aging) when the Zn content was $\geq$ 3 wt% (Zn/Mg ratio 0.6 – 0.8). The chemical composition of precursors after pre-aging (24 h at 90 °C) was found to have a major impact on their capability for subsequent development. Because T-phase evolves in a gradual manner, precursors with

compositions similar to the next evolution stage can transform more easily, thus rendering overall alloy composition a key factor in optimizing hardening behavior [141]. Based on scanning transmission electron microscopy (STEM) investigations into the AlMg5.1Zn3.0Cu0.15 alloy under different aging conditions, Hou et al. [105] proposed that the precipitation sequence of Cu-containing T-phase follows:

SSSS → GPI zone (fully coherent) → GPII zone (T'', fully coherent) → intermediate T' (semi-coherent) → equilibrium T (incoherent) [105]

Hardening upon pre-aging (24 h at 90 °C) was attributed to two types of small, coherent solute agglomerations. While smallest solute agglomerations caused no electron-diffraction signal, a distinct structure was observed for larger ones; they were denoted as GPI and GPII (T''), respectively. Similar particles were also found after extensive natural aging but were present in smaller sizes and higher number density. Upon subsequent artificial aging at higher temperatures, pre-aged samples exhibited a significant increase in hardness, while the strength of natural aged samples declined, indicating that a certain critical particle size (between 1.5 and 2.5 nm) is required for subsequent growth and development into T'- and T-precipitates [105]. Investigations on related alloys (AlMg4.7Zn3.6 with and without 0.6 wt% Cu) had similar results [106] and support the findings by Hou et al. [105]. It was also discovered that precursors require both a critical size of roughly 700 atoms and a complex local chemistry (Mg/(Zn + Cu) ratio $\geq$ 0.7) to develop into T'-precipitates during the second high-temperature aging stage (185 °C) [106].

Because Cu diffusion is limited in the aluminum matrix at lower temperatures [41,142], post-pre-aging precursors contain low amounts of Cu and high amounts of Zn [97]. However, the smallest clusters (initial nuclei) are observed to exhibit a much higher Cu/Zn ratio compared to the majority of precursors formed during the pre-aging procedure [97]. In the absence of Cu, the number density of precursors is significantly lower, which produces a slower and less pronounced hardening response upon subsequent high-temperature aging [106,119,124]. It is assumed that Cu (even in low quantities) promotes nucleation of clusters in the earlier stages of pre-aging, which is similar to the effects observed in Cu-containing AlMg [59,60] and AlZnMg alloys [143]. Meanwhile, DFT calculations [106] revealed that adding Cu neither promotes nor hinders early-stage cluster formation, but that it significantly decreases the formation energy of η'- and, to an even greater extent, T-phase. Based on the chemical composition of post-pre-aging precursors in an AlMg4.7Zn3.6Cu0.6 alloy found by complementary APT analysis it was suggested that transient η' might act as a surrogate phase in T-phase development [106]. In addition to an enhanced formation trend, Cu was also found to improve the thermal stability and strengthening ability of subsequent precursors [106,124]. In consequence, Cu-containing precursors in high density are stable enough to grow and develop during high-temperature aging and to prevent extensive formation of precipitate free zones (PFZ) adjacent to grain boundaries, thus resulting in increased strength [118] and improved resistance to intergranular corrosion [124].

Pan et al. [135] examined the effect of an increasing (Zn + Cu)/Mg ratio (0.63, 0.71, 0.85, 0.97 and 1.21) on the double-step hardening response and the IGC resistance of AlMgZn(Cu) alloys. Peak hardness was observed to shift to earlier aging times and higher levels if the (Zn + Cu)/Mg ratio was increased up to 0.97 due to the decreased size, increased number density and higher volume fraction of Cu-incorporated T-phase. The lattice spacing of the hardening phase gradually decreases with the (Zn + Cu)/Mg ratio as a result of the corresponding substitution of Al by Zn and Cu, thus increasing its thermal stability and hardenability. Simultaneously the IGC resistance was improved, which is attributed to smaller differences in galvanic potential between grain boundary precipitates (GBP) and the matrix [135].

Variations in Mg content (3.5 – 5.6 wt%) were also observed to have a major impact on the mechanical performance of AlMgZn(Cu) alloys. Higher Mg levels have been found to increase the overall strength level which is attributed to increased grain boundary strengthening due to a smaller grain size after solution annealing and an enhanced solid solution strengthening due to higher supersaturation of Mg in the matrix [144]. IGC resistance decreased with increasing Mg (especially at levels higher than 4.6 wt% [145]), but can be improved by a pre-treatment at temperatures close to the solvus temperature of the T-phase prior to artificial aging due to alterations in grain boundary occupancy without major deterioration of achievable peak strength [146]. A similar trend was observed for the susceptibility to stress corrosion cracking (SCC), proving that lower Mg levels are more beneficial due to inhibited anodic dissolution of grain boundary precipitates [147]. Experiments investigating exfoliation corrosion (EXC) in an AlMg4.6Zn3.1Cu0.15 alloy in T6-condition revealed a strong correlation between the alloy's susceptibility to EXC and its subgrain microstructure. Even though EXC seems to be inevitable if grain boundary precipitates (GBP) are present, a lower proportion of subgrain stripes (adjustable via adequate processing) improves EXC resistance [148].

Besides the outstanding hardenability of AlMgZn(Cu) alloys, recent studies have also revealed that adjusted additions of Zn and Cu are capable of limiting Lüders elongation [126] and serrated flow [149] in the pre-aged condition (80 °C/12 h). This has been attributed to a lower effective Mg content in the matrix available for Mg/dislocation interactions, due to its consumption by precipitate formation during pre-aging. Additionally, alloys optimized for fast hardening exhibit the onset of serrated flow at higher strain levels than in non-optimized alloys. While this benefit is more pronounced at low strain rates ($1.7 \times 10^{-4}\ s^{-1}$), it tends to diminish at high strain rates ($3.3 \times 10^{-3}\ s^{-1}$) [149].

Because AlMgZn(Cu) crossover alloys seem to offer beneficial properties for use as construction material, their weldability is a key factor for any broad industrial application in this sector. Investigations by Zhang et al. [150,151] revealed a similarly low liquation cracking tendency of low-Cu (0.15 wt%) alloys exhibiting a Zn/Mg ratio < 1 in peak-aged condition (90 °C/24 h + 140 °C/24 h) when compared to commercial AlMg alloys during fusion welding. Improved weldability is attributed to a lower difference in solid fraction (precipitates) between fusion zone (FZ) and partially melted zone (PMZ) during the solidification stage than that of Cu-free alloys with Zn/Mg ratios > 1, thus offering a better crack healing ability due to a higher liquid metal fraction in the PMZ [150,151]. Follow-up research by Pan et al. [152] revealed a similar trend for AlMgZn(Cu) alloys with higher Cu content (1 wt%, Cu/Mg ratio $\leq$ 0.25). The

superior hot cracking tendency compared to a commercial 7075 alloy (1.6 wt% Cu, Mg/Zn ratio $\geq$ 2.4, Cu/Mg ratio $\geq$ 0.6) has been similarly attributed to a lower number of micro cracks in the weld due to a lower stress concentration at the end of solidification caused by a narrower solidification temperature interval and an increased liquid metal fraction at the terminal stage of welding [152].

AlMgZn(Cu) alloys have also been found to be suitable for joining operations by friction stir welding (FSW). Due to their hardenability by T-phase precipitation, FSW joints offer significantly higher strength compared to commercial AlMg alloys if an adequate post-weld-heat treatment (PWHT) is applied. The deterioration of elongation observed has been attributed to the extensive coarsening of precipitates in the heat affected zone (HAZ) due to the increased temperature during FSW [153].

As a result of their low hot cracking tendency, AlMgZn(Cu) alloys were also tested for application in a wire arc additive manufacturing (WAAM) process. After post-WAAM heat treatment specimens were observed to offer beneficial mechanical performance, thus verifying their suitability for WAAM processing [154,155].

6. Summary

A complex and longstanding challenge for the metallurgy of lightweight non-ferrous alloys is the trade-off between good formability and high strengthening potential. Here existing technological solutions based on aluminum alloys have several limitations, and the development of new alloy design strategies and concepts at the frontier of current scientific knowledge is called for. Today this challenge is also linked to the development of materials for a sustainable future, with an initial focus on lightweight automotive or other traditional transportation applications which will reduce greenhouse gas emissions. However, it has become apparent that the range of applications also – unexpectedly – includes a new class of space materials.

Merging the most beneficial properties of existing commercial aluminum alloys has laid the foundation for a new aluminum alloy design strategy known as crossover alloying. The state of the art of the most recent work and conclusions in this new field of research have been thoroughly reviewed above, and can be summarized as follows.

(i) AlMgCu crossover alloys can limit or even compensate for the undesired strength drop upon paint baking of cold-deformed commercial AlMg alloys. However, the level of compensation is strongly dependent on the level of deformation and processing applied.
(ii) AlMgZn crossover alloys with low Zn content offer improved corrosion resistance due to the suppression of corrosion-prone β-phase at grain boundaries in favor of homogeneously distributed T-phase particles. At increased Zn levels and if adequate processing is applied, surface deterioration by Lüders band and serrated flow is limited and a significant hardening capability by T-phase precipitation can be established.
(iii) If the alloy composition and its processing are carefully matched and optimized, AlMgZn(Cu) crossover alloys can provide an even greater strengthening potential, almost reaching the levels of commercial high-strength AlZnMg(Cu) alloys, and enhanced corrosion resistance compared to Cu-free AlMgZn crossover alloys. Given the state-of-the-art, the crossover alloys herein reviewed are capable of providing good formability, which appears to be similar to or even better than that of commercially available alloys. Nevertheless, it must be mentioned that further experimental data is still limited in this field and more research is required.

Therefore, crossover alloys have the potential to outperform existing commercial aluminum alloys in areas where mechanical strength and corrosion are (for example) the major engineering criteria. Further, because the available research provides strong indications of the feasibility of combining high strengthening ability and good formability in a single alloy system, crossover alloys may be a suitable way to reduce the wide variety of materials deployed for lightweighting, thus contributing to a more sustainable life cycle in the traffic and transportation sectors. According to the facts and scientific evidence presented in this review this class of alloys also has enormous potential for further scientific investigation and subsequent technological development, which may pave the way for the consolidation of an entirely new commercial aluminum alloy class. In addition, controlled alloying with Cu, Zn or Cu + Zn is believed to significantly improve the recyclability of the crossover alloys. This aspect needs to be further evaluated, as it is a criterion of paramount importance to address the current requirements of circular economy.

Even though the current results are promising, further research is required to exploit the full potential of aluminum crossover alloys. This research should not be limited to the crossover between 5xxx/2xxx and 5xxx/7xxx as reviewed here, but should possibly cover the entire aluminum alloy spectrum.

CRediT authorship contribution statement

Lukas Stemper: Conceptualization, Visualization, Writing – original draft. **Matheus A. Tunes:** Writing – review & editing. **Ramona Tosone:** Writing – review & editing. **Peter J. Uggowitzer:** Supervision, Writing – review & editing. **Stefan Pogatscher:** Project administration, Conceptualization, Supervision, Writing – review & editing.

Declaration of Competing Interest

The authors declare that they have no known competing financial interests or personal relationships that could have appeared to influence the work reported in this paper.

Acknowledgements

The financial support by the Austrian Federal Ministry for Digital and Economic Affairs, the National Foundation for Research, Technology and Development and the Christian Doppler Research Association is gratefully acknowledged. The authors also express their sincere thanks to AMAG rolling GmbH for financial support. MAT acknowledges current support from the Laboratory Directed Research and Development (LDRD) program of the Los Alamos National Laboratory under the project number 20200689PRD2. MAT expresses thanks for previous support from the European Research Council (ERC) excellent science grant "TRANSDESIGN" through the Horizon 2020 program under contract 757961 and the Austrian Research Promotion Agency (FFG) within project 3DnanoAnalytics (FFG-No. 858040).

References

[1] European Environment Agency. *Every breath we take*: Improving air quality in Europe. Luxembourg: Publ. Off. of the Europ. Union; 2013.
[2] European Environment Agency, Dejean, F., Greenhouse gas emission trends and projections in Europe 2009, Greenhouse gas emission trends and projections in Europe tracking progress towards Kyoto targets 9, 2009.
[3] Hirsch J. Recent development in aluminium for automotive applications. Trans Nonferrous Met Soc China 2014;24(7):1995–2002. https://doi.org/10.1016/S1003-6326(14)63305-7.
[4] Hirsch J. Aluminium in innovative light-weight car design. Mater Trans 2011;52(5):818–24. https://doi.org/10.2320/matertrans.L-MZ201132.
[5] Adib A, Shadmand MB, Shamsi P, Afridi KK, Amirabadi M, Fateh F, et al. E-mobility — advancements and challenges. IEEE Access 2019;7:165226–40. https://doi.org/10.1109/Access.628763910.1109/ACCESS.2019.2953021.
[6] Olabi AG, Wilberforce T, Abdelkareem MA. Fuel cell application in the automotive industry and future perspective. Energy 2021;214:118955. https://doi.org/10.1016/j.energy.2020.118955.
[7] Yang L, Yu B, Yang Bo, Chen H, Malima G, Wei Y-M. Life cycle environmental assessment of electric and internal combustion engine vehicles in China. J Cleaner Prod 2021;285:124899. https://doi.org/10.1016/j.jclepro.2020.124899.
[8] Held T, Gerrits L. On the road to electrification – A qualitative comparative analysis of urban e-mobility policies in 15 European cities. Transp Policy 2019;81:12–23. https://doi.org/10.1016/j.tranpol.2019.05.014.
[9] Van Mierlo J, Timmermans J-M, Maggetto G, Van den Bossche P, Meyer S, Hecq W, et al. Environmental rating of vehicles with different alternative fuels and drive trains: a comparison of two approaches. Transp Res Part D: Transport Environ 2004;9(5):387–99. https://doi.org/10.1016/j.trd.2004.08.005.
[10] W. Miller, L. Zhuang, J. Bottema, A. Wittebrood, P. de Smet, A. Haszler, A. Vieregge, Recent development in aluminium alloys for the automotive industry, Mater. Sci. Eng., A 280 (2000) 37–49, https://doi.org/10.1016/S0921-5093(99)00653-X.
[11] Morita A. Aluminum alloys for automobile applications. Proc 6th ICAA 1998;1:25–32.
[12] Sivanur K, Umananda KV, Pai D. Advanced materials used in automotive industry-a review. In: Proceedings of the 14th Asia-Pacific Physics Conference, AIP Publishing, 2021, p. 20032.
[13] Carle D, Blount G. The suitability of aluminium as an alternative material for car bodies. Mat Des 1999;20(5):267–72. https://doi.org/10.1016/S0261-3069(99)00003-5.
[14] Raabe D, Tasan CC, Olivetti EA. Strategies for improving the sustainability of structural metals. Nature 2019;575(7781):64–74. https://doi.org/10.1038/s41586-019-1702-5.
[15] Cui Jirang, Roven, H.J., Recycling of automotive aluminum. Trans Nonferrous Met Soc China 20 (2010) 2057–2063, https://doi.org/10.1016/S1003-6326(09)60417-9.
[16] Das SK, Green JAS, Kaufman JG. The development of recycle-friendly automotive aluminum alloys. JOM 2007;59(11):47–51. https://doi.org/10.1007/s11837-007-0140-2.
[17] Buchner H, Laner D, Rechberger H, Fellner J. Potential recycling constraints due to future supply and demand of wrought and cast Al scrap—A closed system perspective on Austria. Resour Conserv Recycl 2017;122:135–42. https://doi.org/10.1016/j.resconrec.2017.01.014.
[18] Ostermann F. *Anwendungstechnologie Aluminium*, Springer, Berlin Heidelberg. Berlin/Heidelberg 2014. https://doi.org/10.1007/978-3-662-05788-9.
[19] Schuster P, Österreicher J, Kirov G, Sommitsch C, Kessler O, Mukeli E. Characterisation and comparison of process chains for producing automotive structural parts from 7xxx aluminium sheets. Metals 2019;9:305. https://doi.org/10.3390/met9030305.
[20] Geiger M, Merklein M. Sheet metal forming - a new kind of forge for the future. Key Eng Mater 2007;344:9–20. https://doi.org/10.4028/www.scientific.net/KEM.344.9.
[21] Zheng K, Politis DJ, Wang L, Lin J. A review on forming techniques for manufacturing lightweight complex—shaped aluminium panel components. Int J Lightweight Mater Manufacture 2018;1(2):55–80. https://doi.org/10.1016/j.ijlmm.2018.03.006.
[22] Jain M, Allin J, Bull MJ. Deep drawing characteristics of automotive aluminum alloys. Mater Sci Eng, A 256 1998;256(1-2):69–82. https://doi.org/10.1016/S0921-5093(98)00845-4.
[23] Ma K, Wen H, Hu T, Topping TD, Isheim D, Seidman DN, et al. Mechanical behavior and strengthening mechanisms in ultrafine grain precipitation-strengthened aluminum alloy. Acta Mater 2014;62:141–55. https://doi.org/10.1016/j.actamat.2013.09.042.
[24] Fang HC, Chao H, Chen KH. Effect of Zr, Er and Cr additions on microstructures and properties of Al–Zn–Mg–Cu alloys. Mater Sci Eng, A 610 2014:10–6. https://doi.org/10.1016/j.msea.2014.05.021.
[25] Feng Chun, Shou Wen-bin, Liu Hui-qun, Yi Dan-qing, Feng Yao-rong. Microstructure and mechanical properties of high strength Al–Zn–Mg–Cu alloys used for oil drill pipes. Trans Nonferrous Met Soc China 2015;25(11):3515–22. https://doi.org/10.1016/S1003-6326(15)63994-2.
[26] Chen Zhiguo, Yuan Zhengui, Ren Jieke. The mechanism of comprehensive properties enhancement in Al–Zn–Mg–Cu alloy via novel thermomechanical treatment. J Alloy Compd 2020;828:154446. https://doi.org/10.1016/j.jallcom.2020.154446.
[27] Chiu Yang-Chun, Du Kun-Ting, Bor Hui-Yun, Liu Guang-Hui, Lee Sheng-Long. The effects of Cu, Zn and Zr on the solution temperature and quenching sensitivity of Al–Zn–Mg–Cu alloys. Mater Chem Phys 2020;247:122853. https://doi.org/10.1016/j.matchemphys.2020.122853.
[28] Zhao Juangang, Liu Zhiyi, Bai Song, Zeng Diping, Luo Lei, Wang Jian. Effects of natural aging on the formation and strengthening effect of G.P. zones in a retrogression and re-aged Al–Zn–Mg–Cu alloy. J Alloys Compounds 829 2020;829:154469. https://doi.org/10.1016/j.jallcom.2020.154469.
[29] Li Bo, Pan Qing-lin, Chen Cong-ping, Yin Zhi-min. Effect of aging time on precipitation behavior, mechanical and corrosion properties of a novel Al-Zn-Mg-Sc-Zr alloy. Trans Nonferrous Met Soc China 2016;26(9):2263–75. https://doi.org/10.1016/S1003-6326(16)64347-9.
[30] Li Hai, Qingzhong Mao, Wang Zhixiu, Miao Fenfen, Fang Bijun, Song Renguo, et al. Simultaneously enhancing the tensile properties and intergranular corrosion resistance of Al–Mg–Si–Cu alloys by a thermo-mechanical treatment. Mater Sci Eng, A 617 2014;617:165–74. https://doi.org/10.1016/j.msea.2014.08.045.
[31] Huo WT, Shi JT, Hou LG, Zhang JS. An improved thermo-mechanical treatment of high-strength Al–Zn–Mg–Cu alloy for effective grain refinement and ductility modification. J Mater Process Technol 2017;239:303–14. https://doi.org/10.1016/j.jmatprotec.2016.08.027.
[32] Polmear IJ, Pons G, Barbaux Y, Octor H, Sanchez C, Morton AJ, et al. After concorde. Mater Sci Technol 2013;15:861–8. https://doi.org/10.1179/026708399101506599.
[33] Li J-F, Ye Z-H, Liu D-Y, Chen Y-L, Zhang X-H, Xu X-Z, Zheng Z-Q. Influence of pre-deformation on aging precipitation behavior of three Al–Cu–Li alloys. Acta Metall Sin (Engl Lett) 30 (2017) 133–145, https://doi.org/10.1007/s40195-016-0519-6.

[34] Zhao YL, Yang ZQ, Zhang Z, Su GY, Ma XL. Double-peak age strengthening of cold-worked 2024, aluminum alloy. Acta Mater 2013;61:1624–38. https://doi.org/10.1016/j.actamat.2012.11.039.

[35] Cheng S, Zhao YH, Zhu YT, Ma E. Optimizing the strength and ductility of fine structured 2024, Al alloy by nano-precipitation. Acta Mater 2007;55:5822–32. https://doi.org/10.1016/j.actamat.2007.06.043.

[36] Huang YJ, Chen ZG, Zheng ZQ. A conventional thermo-mechanical process of Al–Cu–Mg alloy for increasing ductility while maintaining high strength. Scr Mater 2011;64(5):382–5. https://doi.org/10.1016/j.scriptamat.2010.10.037.

[37] Xiao DH, Wang JN, Ding DY, Chen SP. Effect of Cu content on the mechanical properties of an Al–Cu–Mg–Ag alloy. J Alloy Compd 2002;343(1-2):77–81. https://doi.org/10.1016/S0925-8388(02)00076-2.

[38] Li Hai, Mao Qingzhong, Wang Zhixiu, Miao Fenfen, Fang Bijun, Zheng Ziqiao. Enhancing mechanical properties of Al–Mg–Si–Cu sheets by solution treatment substituting for recrystallization annealing before the final cold-rolling. Mater Sci Eng, A 620 2015;620:204–12. https://doi.org/10.1016/j.msea.2014.10.012.

[39] Zhong Hao, Rometsch Paul A, Cao Lingfei, Estrin Yuri. The influence of Mg/Si ratio and Cu content on the stretch formability of 6xxx aluminium alloys. Mater Sci Eng, A 651 2016;651:688–97. https://doi.org/10.1016/j.msea.2015.11.016.

[40] Zhong Hao, Rometsch Paul A, Wu Xiaodong, Cao Lingfei, Estrin Yuri. Influence of pre-ageing on the stretch formability of Al-Mg-Si automotive sheet alloys. Mater Sci Eng, A 697 2017;697:79–85. https://doi.org/10.1016/j.msea.2017.05.009.

[41] Guo MX, Zhang YD, Li GJ, Jin SB, Sha G, Zhang JS, et al. Solute clustering in Al-Mg-Si-Cu-(Zn) alloys during aging. J Alloy Compd 2019;774:347–63. https://doi.org/10.1016/j.jallcom.2018.09.309.

[42] Wang X, Guo M, Zhang J, Zhuang L. Effect of Zn addition on the microstructure, texture evolution and mechanical properties of Al-Mg-Si-Cu alloys. Mater Sci Eng, A 2016;677:522–33. https://doi.org/10.1016/j.msea.2016.09.084.

[43] Cai Yuan-hua, Wang Cong, Zhang Ji-shan. Microstructural characteristics and aging response of Zn-containing Al-Mg-Si-Cu alloy. Int J Miner Metall Mater 2013;20(7):659–64. https://doi.org/10.1007/s12613-013-0780-x.

[44] Glöckel Felix, Uggowitzer Peter J, Felfer Peter, Pogatscher Stefan, Höppel Heinz Werner. Influence of Zn and Sn on the precipitation behavior of new Al-Mg-Si alloys. Materials 2019;12(16):2547. https://doi.org/10.3390/ma12162547.

[45] Hirth S, Marshall G, Court S, Lloyd D. Effects of Si on the aging behaviour and formability of aluminium alloys based on AA6016. Mater Sci Eng, A 319-321 (2001) 452–456, https://doi.org/10.1016/S0921-5093(01)00969-8.

[46] Guo MX, Sha G, Cao LY, Liu WQ, Zhang JS, Zhuang LZ. Enhanced bake-hardening response of an Al–Mg–Si–Cu alloy with Zn addition. Mater Chem Phys 2015;162:15–9. https://doi.org/10.1016/j.matchemphys.2015.07.033.

[47] Naronikar Aditya H, Jamadagni HN Akshay, Simha Amruthamshu, Saikiran B. Optimizing the heat treatment parameters of Al-6061 required for better formability. Mater Today: Proc 2018;5(11):24240–7. https://doi.org/10.1016/j.matpr.2018.10.219.

[48] Yan Lizhen, Li Zhihui, Zhang Yong-an, Xiong Baiqing, Li Xiwu, Liu Hongwei, et al. Pre-aging on early-age behavior and bake hardening response of an Al-0.90Mg-0.80Si-0.64Zn-0.23Cu alloy. Prog Natural Sci: Mater Int 2016;26(4):398–403. https://doi.org/10.1016/j.pnsc.2016.06.005.

[49] Horváth G, Chinh NQ, Gubicza J, Lendvai J. Plastic instabilities and dislocation densities during plastic deformation in Al–Mg alloys. Mater Sci Eng, A 2007;445–446:186–92. https://doi.org/10.1016/j.msea.2006.09.019.

[50] Ryen O, Holmedal B, Nes E. *Workhardening of non-heat treatable aluminum alloys towards large strains*, in. VIR [*] Conference 2004:743–7.

[51] Sylwestrowicz W, Hall EO. The deformation and ageing of mild steel. Proc Phys Soc London, Sect B 1951;64(6):495–502.

[52] Portevin A, Le Chatelier F. Sur un phénomène observé lors de l'essai de traction d'alliages en cours de transformation. Comptes Rendus de l'Académie des Sciences Paris 1923;176:507–10.

[53] Sanders RE, Baumann SF, Stumpf HC. Non-heat-treatable aluminum alloys. Aluminum Alloys: Their Physical and Mechanical Properties 1986;3:1441–84.

[54] Falkenstein H-P, Gruhl W. Forming behavior of aluminum. Bander-Bleche- Rohre 1978;19:265–8.

[55] Lee Byeong-Hyeon, Kim Sung-Hoon, Park Jun-Hyoung, Kim Hyung-Wook, Lee Jae-Chul. Role of Mg in simultaneously improving the strength and ductility of Al–Mg alloys. Mater Sci Eng, A 657 2016;657:115–22. https://doi.org/10.1016/j.msea.2016.01.089.

[56] Tunes Matheus A, Stemper Lukas, Greaves Graeme, Uggowitzer Peter J, Pogatscher Stefan. Prototypic lightweight alloy design for stellar-radiation environments. Adv Sci 2020;7(22):2002397. https://doi.org/10.1002/advs.v7.2210.1002/advs.202002397.

[57] Tunes MA, Quick CR, Stemper L, Coradini DSR, Grasserbauer J, Dumitraschkewitz P, Kremmer TM, Pogatscher S. A fast and implantation-free sample production method for large scale electron-transparent metallic samples destined for MEMS-based in situ S/TEM experiments. Materials (Basel, Switzerland) 14 (2021), https://doi.org/10.3390/ma14051085.

[58] Hino M, Koga S, Oie S, Yanagawa M. Properties of Al-Mg Based Alloys for Automobile Body Panel. Kobelco Technology Review 1991.

[59] Ratchev P, Verlinden B, De Smet P, Van Houtte P. Precipitation hardening of an Al–4.2wt% Mg–0.6wt% Cu alloy. Acta Mater 1998;46(10):3523–33.

[60] Ratchev P, Verlinden B, de Smet P, van Houtte P. Artificial ageing of Al–Mg–Cu alloys. Mater Trans 1999;34–41.

[61] Ringer Simon P, Hono Kazuhiro, Sakurai Toshio, Polmear Ian J. Cluster hardening in an aged Al-Cu-Mg alloy. Scr Mater 1997;36(5):517–21.

[62] Marceau RKW, Sha G, Ferragut R, Dupasquier A, Ringer SP. Solute clustering in Al–Cu–Mg alloys during the early stages of elevated temperature ageing. Acta Mater 2010;58(15):4923–39. https://doi.org/10.1016/j.actamat.2010.05.020.

[63] Bourgeois Laure, Chen Yiqiang, Zhang Zezhong, Zhang Yong, Medhekar Nikhil. Direct solid-state nucleation from preexisting coherent precipitates in aluminium. Microsc Microanal 2017;23(S1):430–1. https://doi.org/10.1017/S1431927617002835.

[64] Wang SC, Starink MJ. Two types of S phase precipitates in Al–Cu–Mg alloys. Acta Mater 2007;55(3):933–41. https://doi.org/10.1016/j.actamat.2006.09.015.

[65] Charai A, Walther T, Alfonso C, Zahra A-M, Zahra CY. Coexistence of clusters, GPB zones, S″-, S′- and S-phases in an Al–0.9% Cu–1.4% Mg alloy. Acta Mater 2000;48(10):2751–64. https://doi.org/10.1016/S1359-6454(99)00422-X.

[66] Kovarik L, Gouma PI, Kisielowski C, Court SA, Mills MJ. A HRTEM study of metastable phase formation in Al–Mg–Cu alloys during artificial aging. Acta Mater 2004;52(9):2509–20. https://doi.org/10.1016/j.actamat.2004.01.041.

[67] Kovarik L, Gouma PI, Kisielowski C, Court SA, Mills MJ. Decomposition of an Al–Mg–Cu alloy—a high resolution transmission electron microscopy investigation. Mater Sci Eng, A 387-389 (2004) 326–330, https://doi.org/10.1016/j.msea.2004.03.087.

[68] Kovarik L, Miller MK, Court SA, Mills MJ. Origin of the modified orientation relationship for S(S″)-phase in Al–Mg–Cu alloys. Acta Mater 2006;54(7):1731–40. https://doi.org/10.1016/j.actamat.2005.11.045.

[69] Chen Xuanliang, Marioara Calin D, Andersen Sigmund J, Friis Jesper, Lervik Adrian, Holmestad Randi, et al. Precipitation processes and structural evolutions of various GPB zones and two types of S phases in a cold-rolled Al-Mg-Cu alloy. Mater Des 2021;199:109425. https://doi.org/10.1016/j.matdes.2020.109425.

[70] Alil A, Popović M, Radetić T, Zrilić M, Romhanji E. Influence of annealing temperature on the baking response and corrosion properties of an Al–4.6wt% Mg alloy with 0.54wt% Cu. J Alloys Compd 2015;625:76–84. https://doi.org/10.1016/j.jallcom.2014.11.063.

[71] Engler O, Marioara CD, Hentschel T, Brinkman H-J. Influence of copper additions on materials properties and corrosion behaviour of Al–Mg alloy sheet. J Alloys Compd 2017;710:650–62. https://doi.org/10.1016/j.jallcom.2017.03.298.

[72] Medrano S, Zhao H, Gault B, De Geuser F, Sinclair CW. A model to unravel the beneficial contributions of trace Cu in wrought Al-Mg alloys. Acta Mater 2021;208:116734. https://doi.org/10.1016/j.actamat.2021.116734.

[73] Medrano S, Zhao H, De Geuser F, Gault B, Stephenson LT, Deschamps A, et al. Cluster hardening in Al-3Mg triggered by small Cu additions. Acta Mater 2018;161:12–20. https://doi.org/10.1016/j.actamat.2018.08.050.

[74] Pogatscher S, Antrekowitsch H, Leitner H, Ebner T, Uggowitzer PJ. Mechanisms controlling the artificial aging of Al–Mg–Si Alloys. Acta Mater 2011;59(9):3352–63. https://doi.org/10.1016/j.actamat.2011.02.010.

[75] Werinos M, Antrekowitsch H, Ebner T, Prillhofer R, Curtin WA, Uggowitzer PJ, et al. Design strategy for controlled natural aging in Al–Mg–Si alloys. Acta Materialia 118 2016;118:296–305. https://doi.org/10.1016/j.actamat.2016.07.048.

[76] Schmid Florian, Uggowitzer Peter J, Schäublin Robin, Werinos Marion, Ebner Thomas, Pogatscher Stefan. Effect of thermal treatments on Sn-alloyed Al-Mg-Si alloys. Materials 2019;12(11):1801. https://doi.org/10.3390/ma12111801.

[77] Prillhofer R, Rank G, Berneder J, Antrekowitsch H, Uggowitzer PJ, Pogatscher S. Property criteria for automotive Al-Mg-Si sheet alloys. Materials 2014;7:5047–68. https://doi.org/10.3390/ma7075047.

[78] Green W Paul, Kulas Mary-Anne, Niazi Amanda, Taleff Eric M, Oishi Keiichiro, Krajewski Paul E, et al. Deformation and failure of a superplastic AA5083 aluminum material with a cu addition. Metall Mater Trans A 2006;37(9):2727–38. https://doi.org/10.1007/BF02586106.

[79] Ebenberger P, Uggowitzer PJ, Gerold B, Pogatscher S. Effect of compositional and processing variations in new 5182-type AlMgMn alloys on mechanical properties and deformation surface quality. Materials (Basel, Switzerland) 12 (2019), https://doi.org/10.3390/ma12101645.

[80] Zhang Z-R, van Houtte P, Verlinden B. Influence of previous ageing treatments on the strength of an Al-4.3 wt.% Mg-1.2 wt.% Cu alloy processed by ECAE. IJMR 2008;99:273–80. https://doi.org/10.3139/146.101633.

[81] Vidal V, Zhang ZR, Verlinden B. Precipitation hardening and grain refinement in an Al–4.2wt%Mg–1.2wt%Cu processed by ECAP. J Mater Sci 2008;43(23-24):7418–25. https://doi.org/10.1007/s10853-008-2746-3.

[82] Löffler H, Kovcs I, Lendvai J. Decomposition processes in Al-Zn-Mg alloys. J Mater Sci 1983;18(8):2215–40. https://doi.org/10.1007/BF00541825.

[83] Köster W, Dullenkopf W. The Al-Mg-Zn ternary system. III. The partial region Mg-Al3Mg4-Al2Mg3Zn3-MgZn2-Mg'. Z Metallkd 1936;28:363–7.

[84] Köster W, Wolf W. The Al-Mg-Zn ternary system. I. The Al-Al2Mg3Zn3-MgZn2-Zn region. Z Metallkd 1936;28:155–8.

[85] Fridlyander IN, Gerchikova NS, Zaitseva NI. Kinetics of aging of alloy V92Ts of the Al- Zn- Mg system. Metalloved Term Obrab Met 1966;8:11.

[86] Schmalzried H, Gerold V. Age-hardening in an Al–Mg–Zn alloy. Z Metallkd 1958;49:291–301.

[87] Graf R. An X-ray study of the precipitation phenomenon in an Al—Zn—Mg alloy with 9% Zn and 1% Mg (AZ 9 Gl). Compt rend 1957;244:337.

[88] Saulnier A, Cabane G. Recherches récentes sur les alliages Al-Zn-Mg-Cu. Revue de Métallurgie 1949;46(1):13–23.

[89] Mondolfo LF. Structure of the aluminium: magnesium: zinc alloys. Metallurgical Reviews 1971;16(1):95–124. https://doi.org/10.1179/mtlr.1971.16.1.95.

[90] Inoue H, Sato T, Kojima Y, Takahashi T. The temperature limit for GP zone formation in an Al-Zn-Mg alloy. Metall and Mat Trans A 1981;12(8):1429–34. https://doi.org/10.1007/BF02643687.

[91] Zou Yan, Wu Xiaodong, Tang Songbai, Zhu Qianqian, Song Hui, Guo Mingxing, et al. Investigation on microstructure and mechanical properties of Al-Zn-Mg-Cu alloys with various Zn/Mg ratios. J Mater Sci Technol 2021;85:106–17. https://doi.org/10.1016/j.jmst.2020.12.045.

[92] Zou Yan, Wu Xiaodong, Tang Songbai, Zhu Qianqian, Song Hui, Cao Lingfei. Co-precipitation of T′ and η′ phase in Al-Zn-Mg-Cu alloys. Mater Charact 2020;169:110610. https://doi.org/10.1016/j.matchar.2020.110610.

[93] Bergman G, Waugh JLT, Pauling L. The crystal structure of the metallic phase Mg32(Al, Zn)49. Acta Cryst 1957;10:254–9. https://doi.org/10.1107/S0365110X57000808.

[94] Villars P, Cenzual K. Mg32(Al,Zn)49 (Mg32Zn31.9Al17.1) Crystal Structure: Datasheet from "PAULING FILE Multinaries Edition - 2012" in SpringerMaterials, Springer-Verlag Berlin Heidelberg & Material Phases Data System (MPDS), Switzerland & National Institute for Materials Science (NIMS), Japan. https://materials.springer.com/isp/crystallographic/docs/sd_1252007.

[95] Strawbridge DJ, Hume-Rothery W, Little AT. The constitution of aluminium copper magnesium zinc alloys at 460-degree-c. J Inst Met 1948;74:191–225.

[96] Belov NA, Eskin DG, Aksenov AA. *Multicomponent phase diagrams*: Applications for commercial aluminum alloys. 1st ed. Amsterdam: Elsevier; 2005.

[97] Cao C, Zhang Di, Zhuang L, Zhang J. Improved age-hardening response and altered precipitation behavior of Al-5.2Mg-0.45Cu-2.0Zn (wt%) alloy with pre-aging treatment. J Alloys Compd 2017;691:40–3. https://doi.org/10.1016/j.jallcom.2016.08.206.

[98] Bigot Annabelle, Auger Pierre, Chambreland Sylvain, Blavette Didier, Reeves Andrew. Atomic scale imaging and analysis of T' precipitates in Al-Mg-Zn alloys. Microsc Microanal Microstruct 1997;8(2):103–13. https://doi.org/10.1051/mmm:1997109.

[99] Afify Nasser, Gaber Abdel-Fattah, Abbady Ghada. Fine scale precipitates in Al-Mg-Zn alloys after various aging temperatures. MSA 2011;02(05):427–34. https://doi.org/10.4236/msa:2011.25056.

[100] Polmear IJ. *Light alloys*: Metallurgy of the light metals. 3rd ed. London: Arnold; 1999.

[101] Polmear, I.J., StJohn, D., Nie, J.-F., Qian, M., Light alloys: Metallurgy of the light metals, Butterworth-Heinemann, Oxford, 2017.

[102] Zeid EF Abo. Influence of aging temperature on precipitation kinetics, morphology and hardening behavior of Al-7475 alloy. Arab J Sci Eng 2019;44(7):6621–9. https://doi.org/10.1007/s13369-019-03825-7.

[103] Yang XB, Chen JH, Liu JZ, Qin F, Xie J, Wu CL. A high-strength AlZnMg alloy hardened by the T-phase precipitates. J Alloys Compd 2014;610:69–73. https://doi.org/10.1016/j.jallcom.2014.04.185.

[104] Huang ZW, Loretto MH, Smallman RE, White J. The mechanism of nucleation and precipitation in 7075–0.7 Li alloy. Acta Metall Mater 1994;42(2):549–59. https://doi.org/10.1016/0956-7151(94)90509-6.

[105] Hou S, Liu P, Zhang Di, Zhang J, Zhuang L. Precipitation hardening behavior and microstructure evolution of Al–5.1 Mg–0.15Cu alloy with 3.0Zn (wt%) addition. J Mater Sci 2018;53:3846–61. https://doi.org/10.1007/s10853-017-1811-1.

[106] Stemper Lukas, Tunes Matheus A, Dumitraschkewitz Phillip, Mendez-Martin Francisca, Tosone Ramona, Marchand Daniel, et al. Giant hardening response in AlMgZn(Cu) alloys. Acta Mater 2021;206:116617. https://doi.org/10.1016/j.actamat.2020.116617.

[107] Berg LK, Gjønnes J, Hansen V, Li XZ, Knutson-Wedel M, Waterloo G, et al. GP-zones in Al–Zn–Mg alloys and their role in artificial aging. Acta Mater 2001;49(17):3443–51. https://doi.org/10.1016/S1359-6454(01)00251-8.

[108] Carroll MC, Gouma PI, Mills MJ, Daehn GS, Dunbar BR. Effects of Zn additions on the grain boundary precipitation and corrosion of Al-5083. Scr Mater 2000;42(4):335–40. https://doi.org/10.1016/S1359-6462(99)00349-8.

[109] Meng C, Zhang Di, Cui H, Zhuang L, Zhang J. Mechanical properties, intergranular corrosion behavior and microstructure of Zn modified Al–Mg alloys. J Alloys Compd 2014;617:925–32. https://doi.org/10.1016/j.jallcom.2014.08.099.

[110] Meng Chun-Yan, Zhang Di, Liu Ping-Ping, Zhuang Lin-Zhong, Zhang Ji-Shan. Microstructure characterization in a sensitized Al–Mg–Mn–Zn alloy. Rare Met 2018;37(2):129–35. https://doi.org/10.1007/s12598-015-0665-4.

[111] Zhao Jing-wei, Luo Bing-hui, He Ke-jian, Bai Zhen-hai, Li Bin, Chen Wei. Effects of minor Zn content on microstructure and corrosion properties of Al−Mg alloy. J Cent South Univ 2016;23(12):3051–9. https://doi.org/10.1007/s11771-016-3368-6.

[112] Meng C, Zhang Di, Zhuang L, Zhang J. Correlations between stress corrosion cracking, grain boundary precipitates and Zn content of Al–Mg–Zn alloys. J Alloys Compd 2016;655:178–87. https://doi.org/10.1016/j.jallcom.2015.09.159.

[113] Xu Xiaojing, Jin Xiaopeng, Liu Zheng, Zhang Bin, Zhang Rikai, Zhuang Yuan, et al. Influence of large amount Zn on mechanical properties and corrosion resistance of 5083 hot rolled aluminum alloy. Appl Phys A 2020;126(9). https://doi.org/10.1007/s00339-020-03908-5.

[114] Matsumoto K, Aruga Y, Tsuneishi H, Iwai H, Mizuno M, Araki H. Effects of Zn addition and aging condition on serrated flow in Al-Mg alloys. Mater Sci Forum 2014;794–796:483–8. https://doi.org/10.4028/www.scientific.net/MSF.794-796.483.

[115] Cao Cheng, Zhang Di, He Zhanbing, Zhuang Linzhong, Zhang Jishan. Enhanced and accelerated age hardening response of Al-5.2Mg-0.45Cu (wt%) alloy with Zn addition. Mater Sci Eng, A 666 2016;666:34–42. https://doi.org/10.1016/j.msea.2016.04.022.

[116] Matsumoto Katsushi, Aruga Yasuhiro, Tsuneishi Hidemasa, Iwai Hikaru, Mizuno Masataka, Araki Hideki. Effects of precipitation state on serrated flow in Al-Mg(-Zn) alloys. Mater Trans 2016;57(7):1101–8. https://doi.org/10.2320/matertrans.L-M2016814.

[117] Yun Juhee, Kang Seungwon, Lee Sangjun, Bae Donghyun. Development of heat-treatable Al-5Mg alloy sheets with the addition of Zn. Mater Sci Eng, A 744 2019;744:21–7. https://doi.org/10.1016/j.msea.2018.11.145.

[118] Stemper Lukas, Mitas Bernhard, Kremmer Thomas, Otterbach Steffen, Uggowitzer Peter J, Pogatscher Stefan. Age-hardening of high pressure die casting AlMg alloys with Zn and combined Zn and Cu additions. Mater Des 2019;181:107927. https://doi.org/10.1016/j.matdes.2019.107927.

[119] Stemper L, Tunes MA, Oberhauser P, Uggowitzer PJ, Pogatscher S. Age-hardening response of AlMgZn alloys with Cu and Ag additions. Acta Mater 2020;195:541–54. https://doi.org/10.1016/j.actamat.2020.05.066.

[120] Verfahren zur Herstellung von magnesium- und zinkhaltigen Aluminium-Legierungs-Blechen, DE 2838543 A1 (1978), Schweizer Aluminium AG.

[121] Zhu Xiangzhen, Liu Fuchu, Wang Shihao, Ji Shouxun. The development of low-temperature heat-treatable high-pressure die-cast Al–Mg–Fe–Mn alloys with Zn. J Mater Sci 2021;56(18):11083–97. https://doi.org/10.1007/s10853-021-05972-5.

[122] Vlach Martin, Cizek Jakub, Kodetova Veronika, Leibner Michal, Cieslar Miroslav, Harcuba Petr, et al. Phase transformations in novel hot-deformed Al–Zn–Mg–Cu–Si–Mn–Fe(–Sc–Zr) alloys. Mater Des 2020;193:108821. https://doi.org/10.1016/j.matdes.2020.108821.

[123] Zhao Huan, Chen Yiqiang, Gault Baptiste, Makineni Surendra Kumar, Ponge Dirk, Raabe Dierk. (Al, Zn)3Zr dispersoids assisted η′ precipitation in anAl-Zn-Mg-Cu-Zr alloy. Materialia 2020;10:100641. https://doi.org/10.1016/j.mtla.2020.100641.

[124] Cao C, Zhang Di, Wang X, Ma Q, Zhuang L, Zhang J. Effects of Cu addition on the precipitation hardening response and intergranular corrosion of Al-5.2Mg-2.0Zn (wt.%) alloy. Mater Charact 2016;122:177–82. https://doi.org/10.1016/j.matchar.2016.11.004.

[125] Cao C, Zhang D, Zhuang L, Zhang J, Liu J. Effect of pre-aging treatment on room temperature stability of Al-5.2Mg-0.45Cu-2.0Zn alloy sheet. Xiyou Jinshu Cailiao Yu Gongcheng/Rare Metal Materials and Engineering 2020;49:1166–70.

[126] Geng Y, Zhang Di, Zhang J, Zhuang L. On the suppression of Lüders elongation in high-strength Cu/Zn modified 5xxx series aluminum alloy. J Alloy Compd 2020:155–1138. https://doi.org/10.1016/j.jallcom.2020.155138.

[127] Mecking H, Kocks UF. Kinetics of flow and strain-hardening. Acta Metall 1981;29(11):1865–75. https://doi.org/10.1016/0001-6160(81)90112-7.

[128] Gruber Belinda, Grabner Florian, Falkinger Georg, Schökel Alexander, Spieckermann Florian, Uggowitzer Peter J, et al. Room temperature recovery of cryogenically deformed aluminium alloys. Mater Des 2020;193:108819. https://doi.org/10.1016/j.matdes.2020.108819.

[129] Taylor GI. The mechanism of plastic deformation of crystals. Proc R Soc Lond A 1934;145:362–87. https://doi.org/10.1098/rspa.1934.0106.

[130] Österreicher JA, Kirov G, Gerstl SS, Mukeli E, Grabner F, Kumar M. Stabilization of 7xxx aluminium alloys. J Alloys Compd 2018;740:167–73. https://doi.org/10.1016/j.jallcom.2018.01.003.

[131] Österreicher Johannes A, Tunes Matheus A, Grabner Florian, Arnoldt Aurel, Kremmer Thomas, Pogatscher Stefan, et al. Warm-forming of pre-aged Al-Zn-Mg-Cu alloy sheet. Mater Des 2020;193:108837. https://doi.org/10.1016/j.matdes.2020.108837.

[132] Omer Kaab, Abolhasani Atekeh, Kim Samuel, Nikdejad Tirdad, Butcher Clifford, Wells Mary, et al. Process parameters for hot stamping of AA7075 and D-7xxx to achieve high performance aged products. J Mater Process Technol 2018;257:170–9. https://doi.org/10.1016/j.jmatprotec.2018.02.039.

[133] Schmid Florian, Dumitraschkewitz Philip, Kremmer Thomas, Uggowitzer Peter J, Tosone Ramona, Pogatscher Stefan. Enhanced aging kinetics in Al-Mg-Si alloys by up-quenching. Commun Mater 2021;2(1). https://doi.org/10.1038/s43246-021-00164-9.

[134] Longgang Hou, Jiajia Yu, Di Zhang, Linzhong Zhuang, Li Zhou, Jishan Zhang. Corrosion behavior of friction stir welded Al-Mg-(Zn) alloys. Rare Metal Mater Eng 2017;46(9):2437–44. https://doi.org/10.1016/S1875-5372(17)30212-6.

[135] Pan Yanlin, Zhang Di, Liu Haoran, Zhuang Linzhong, Zhang Jishan. Precipitation hardening and intergranular corrosion behavior of novel Al–Mg–Zn(-Cu) alloys. J Alloy Compd 2021;853:157199. https://doi.org/10.1016/j.jallcom.2020.157199.

[136] Ma Q, Zhang Di, Zhuang L, Zhang J. Intergranular corrosion resistance of Zn modified 5xxx series Al alloy during retrogression and re-aging treatment. Mater Charact 2018;144:264–73. https://doi.org/10.1016/j.matchar.2018.07.008.

[137] Cina B. Reducing the susceptibility of alloys, particularly aluminium alloys, to stress corrosion cracking. US3856584 1974.

[138] Carroll M, Gouma P, Daehn G, Mills M. Effects of minor Cu additions on a Zn-modified Al-5083 alloy, Mater. Sci. Eng., A 319-321 (2001) 425–428, https://doi.org/10.1016/S0921-5093(00)02021-9.

[139] Carroll MC, Buchheit RG, Daehn GS, Mills MJ. Optimum Trace Copper Levels for SCC Resistance in a Zn-Modified Al-5083 Alloy. Mater Sci Forum 2002;396–402:1443–8. https://doi.org/10.4028/www.scientific.net/MSF.396-402.1443.

[140] Tang Hua-Ping, Wang Qu-Dong, Luo Colin, Lei Chuan, Liu Tian-Wen, Li Zhong-Yang, et al. Effects of aging treatment on the precipitation behaviors and mechanical properties of Al-5.0Mg-3.0Zn-1.0Cu cast alloys. J Alloys Compounds 842 2020;842:155707. https://doi.org/10.1016/j.jallcom.2020.155707.

[141] Hou Shengli, Zhang Di, Ding Qingwei, Zhang Jishan, Zhuang Linzhong. Solute clustering and precipitation of Al-5.1Mg-0.15Cu-xZn alloy. Mater Sci Eng, A 2019;759:465–78. https://doi.org/10.1016/j.msea.2019.05.066.

[142] Du Yong, Chang YA, Huang Baiyun, Gong Weiping, Jin Zhanpeng, Xu Honghui, et al. Diffusion coefficients of some solutes in fcc and liquid Al: critical evaluation and correlation. Mater Sci Eng, A 2003;363(1-2):140–51.

[143] Deschamps A, Bréchet Y, Livet F. Influence of copper addition on precipitation kinetics and hardening in Al–Zn–Mg alloy. Mater Sci Technol 1999;15(9):993–1000. https://doi.org/10.1179/026708399101506832.

[144] Ding Qingwei, Zhang Di, Pan Yanlin, Hou Shengli, Zhuang Linzhong, Zhang Jishan. Strengthening mechanism of age-hardenable Al– x Mg–3Zn alloys. Mater Sci Technol 2019;35(9):1071–80. https://doi.org/10.1080/02670836.2019.1612590.

[145] Ding Q, Zhang Di, Zuo J, Hou S, Zhuang L, Zhang J. The effect of grain boundary character evolution on the intergranular corrosion behavior of advanced Al-Mg-3wt%Zn alloy with Mg variation. Mater Charact 2018;146:47–54. https://doi.org/10.1016/j.matchar.2018.09.044.

[146] Hou Shengli, Zhang Di, Pan Yanlin, Ding Qingwei, Long Weimin, Zhang Jishan, et al. Dependence of microstructure, mechanical properties, and inter-granular corrosion behavior of Al-5.1Mg-3.0Zn-0.15Cu alloys with high temperature pre-treatment. Mater Characterization 2020;168:110512. https://doi.org/10.1016/j.matchar.2020.110512.

[147] Ding Q, Zhang D, Liu H, Zhang J. Stress corrosion cracking behavior of Al-xMg-3.1Zn aluminum alloys and its mechanism. Xiyou Jinshu Cailiao Yu Gongcheng/Rare Metal Mater Eng 2020;49:1601–6.

[148] Ding Q, Di Zhang, Yu Y, Zhuang L, Zhang J. Role of subgrain stripe on the exfoliation corrosion of Al-4.6Mg-3.1wt%Zn (wt.%) alloy, Corrosion Sci (2020) 108622, https://doi.org/10.1016/j.corsci.2020.108622.

[149] Geng Yingxin, Zhang Di, Zhang Jishan, Zhuang Linzhong. Zn/Cu regulated critical strain and serrated flow behavior in Al–Mg alloys. Mater Sci Eng, A 2020;795:139991. https://doi.org/10.1016/j.msea.2020.139991.

[150] Zhang Di, Zhao Xin, Pan Yanlin, Li Hongxiang, Zhou Li, Zhang Jishan, et al. The suppression of solidification cracking of Al welds by regulating Zn/Mg ratio. Weld World 2021;65(4):691–8. https://doi.org/10.1007/s40194-020-01047-2.

[151] Di Zhang, Zhao X, Pan Y, Li H, Zhou L, Zhang J, Zhuang L. Liquation cracking tendency of novel Al-Mg-Zn alloys with a Zn/Mg ratio below 1.0 during fusion welding, Metals 10 (2020) 222, https://doi.org/10.3390/met10020222.

[152] Pan Yanlin, Zhang Di, Liu Haoran, Zhang Zhaorui, Li Hongxiang, Zhuang Linzhong, et al. Reducing welding hot cracking of high-strength novel Al–Mg–Zn–Cu alloys based on the prediction of the T-shaped device. Sci Technol Weld Joining 2020;25(6):483–9. https://doi.org/10.1080/13621718.2020.1746035.

[153] Zhang Di, Wang Xu, Pan Yanlin, Hou Shengli, Zhang Jishan, Zhuang Linzhong, et al. Friction stir welding of novel T-phase strengthened Zn-modified Al–Mg alloy. J Mater Sci 2021;56(8):5283–95. https://doi.org/10.1007/s10853-020-05609-z.

[154] Klein Thomas, Schnall Martin, Gomes Bianca, Warczok Piotr, Fleischhacker Dominik, Morais Paulo J. Wire-arc additive manufacturing of a novel high-performance Al-Zn-Mg-Cu alloy: Processing, characterization and feasibility demonstration. Addit Manuf 2021;37:101663. https://doi.org/10.1016/j.addma.2020.101663.

[155] Morais PJ, Gomes B, Santos P, Gomes M, Gradinger R, Schnall M, Bozorgi S, Klein T, Fleischhacker D, Warczok P, Falahati A, Kozeschnik E. Characterisation of a High-Performance Al-Zn-Mg-Cu Alloy Designed for Wire Arc Additive Manufacturing, Materials (Basel, Switzerland) 13 (2020), https://doi.org/10.3390/ma13071610.